ASIAN JOURNAL OF PHARMACEUTICAL AND CLINICAL RESEARCH

INNOVARE ACADEMIC SCIENCES
Knowledge to Innovation

Vol 19, Issue 4, 2026

Online - 2455-3891
Print - 0974-2441

Research Article

NEUROPROTECTIVE EVALUATION OF TANGERETIN: INSIGHTS FROM *INSILICO* AND *IN VITRO* STUDIES ON RAT GLIOMA CELL LINE

MONICA P[1]*, SRI VARSHINI BAYYANA VN[2], NATTYA PARAMESH[2], THILAK GB[2]

Department of Pharmaceutical Biotechnology, JSS College of Pharmacy, JSS Academy of Higher Education and Research, Udhagamandalam, Tamil Nadu, India. [2]Department of Pharmaceutical Biotechnology, JSS College of Pharmacy, JSS Academy of Higher Education and Research, Udhagamandalam, Tamil Nadu, India.
***Corresponding author: Monica P; Email: monica@jssuni.edu.in**

Received: 31 October 2025, Revised and Accepted: 18 February 2026

ABSTRACT

Objective: The objective of the study is to investigate the neuroprotective effect of tangeretin by *in silico* molecular docking with GluN2B-containing N-methyl-D-aspartic acid (NMDA) receptor and *in vitro* assays using the C6 cell line.

Methods: Phytochemicals sourced from PubChem and the ZINC database were docked to the GluN2B subunit-containing NMDA receptor (NMDAR) (Protein Data Bank: 5EWJ) using PyRx. Absorption, distribution, metabolism, excretion, toxicity properties, and blood–brain barrier (BBB) permeability were assessed through SwissADME and Online BBB prediction server. With the molecule of interest, *in vitro* studies such as MTT, apoptosis assay, gene expression of Bcl-2, Bax-2, caspase-3, and poly(ADP-ribose) polymerase 1 were detected.

Results: The study explored tangeretin as a therapeutic agent targeting the GluN2B subunit of NMDARs. Docking studies showed strong binding affinity (−7.3 kcal/mol) and interactions mimicking ifenprodil. Tangeretin complied with Lipinski's rule, high GI absorption (98.478%), BBB penetration, and non-mutagenicity, supporting its use for neurodegenerative diseases. *In vitro* assays confirmed >85% viability at 1000 µg/mL (85.65 ± 1.07% at 1000 µg/mL) and anti-apoptotic effects by significantly upregulating Bcl-2 and downregulating Bax and Caspase-3.

Conclusion: Tangeretin demonstrated significant neuroprotective potential by inhibiting NMDAR-mediated apoptosis, increasing anti-apoptotic gene expression. With its high gastrointestinal absorption, BBB permeability, and low cytotoxicity, tangeretin emerges as a safe therapeutic candidate for treating neurodegenerative diseases. This study elucidates molecular and cellular effects, laying the foundation for developing tangeretin-based neuroprotective therapies.

Keywords: Neurodegeneration, Apoptosis, Excitotoxicity, N-methyl-D-aspartate receptor inhibitors, Rat glioma cell line.

 DOI: http://dx.doi.org/10.22159/ajpcr.2026v19i4.57347. Journal homepage: https://innovareacademics.in/journals/index.php/ajpcr

INTRODUCTION

The nervous system is an extremely sophisticated organ system that performs a wide range of functions, including receiving and processing sensory information and controlling extremely complex actions that allow for survival. It consists of highly specialized cell types – neurons and its loss is postmitotic, i.e., lost neurons are not replaced. Acute or chronic exposure to neurotoxicants disrupts the neurophysiological functions and leads to neurodegeneration [1]. Etymologically, the word "Neurodegeneration" is composed of the prefix "neuro-," which refers to nerve cells (i.e., neurons), and "degeneration," which refers to a process of losing structure or function. Thus, neurodegeneration describes any pathological condition that causes the loss of neuronal structure and function. The word "Neurodegeneration "describes a wide range of neurological disorders known as neurodegenerative disorders such as Alzheimer's disease (AD), Parkinson's disease, Multiple sclerosis, and amyotrophic lateral sclerosis, which can have fatal effects on mental and physical functioning and represent a serious threat to human beings. These neurodegenerative diseases result in Motor deterioration (deterioration of normal physical activities), Cognitive decline, and dementia (deterioration of memory, thinking, and behavior [2,3]. Several drugs are available that can help manage the symptoms of neurodegenerative diseases, although they do not cure the underlying condition. For example, cholinesterase inhibitors such as donepezil, rivastigmine, galantamine, and memantine are used to manage the cognitive symptoms of AD [4-6]. Furthermore, donepezil's beneficial effect on memory is found to be temporary. The progression of AD has not been modified [6].

Common pathogenic mechanisms in neurodegenerative diseases

Typical pathogenic mechanisms that are shared across various neurodegenerative disorders comprise aggregation and accumulation of abnormal proteins (Amyloidβ and neurofibrillary tangles in the case of AD and Lewy bodies in the case of Parkinson's disease) [7,8]. Genetic mutations (SOD1, parkin, and Huntingtin), neurotrophins dysfunction, oxidative stress and formation of reactive oxygen species (ROS), excitotoxicity: Overactivation of excitatory neurotransmitter receptors impairs calcium homeostasis and activates the synthesis of nitric oxide and formation of free radicals leading to neuronal damage and death, impaired cellular metabolism (mitochondrial dysfunctions and DNA damage) [10], neuroinflammatory process – all of which contribute to neuronal apoptosis [2,3,11,12].

Excitotoxicity

The brain's main excitatory system is made up of glutamatergic neurons, which are essential in synaptic plasticity for learning and memory processes. Glutamate is the key neurotransmitter in basic perception and cognition under normal physiological circumstances, eliciting an excitatory response. This reaction is the result of glutamate interacting with the receptors that are composed of cation channels. "Excitotoxicity" – excessive stimulation of glutamate receptors causes neuronal malfunction and death. Glutamate and glutamatergic activity are overexpressed in several neurodegenerative disorders. Glutamate's excitatory effects are mediated by the activation of three main ionotropic receptors that are activated by glutamate, including kainic acid, α-amino-3-hydroxy-5-methylisoxazole-4-propionate receptors (AMPARs), and N-methyl-D-

aspartic acid (NMDA) receptors (NMDARs). Chronic NMDAR activation leads to the loss of neurons [13]. NMDARs are found in the postsynaptic neurons, which mediate synaptic plasticity and rapid excitatory transmission and act as a main modulator in long-term potentiation and depression. This receptor is permeable to sodium ion, potassium ion, and calcium ion ($ca2^+$), and it is closed by a magnesium ion ($Mg2^+$). Activation of AMPARs removes $Mg2^+$ and the influx of ions happens [14]. Large-scale persistent NMDAR activation, particularly of the NR1/NR2B subtype, raises intracellular calcium influx and catabolic enzyme activity. These changes can set off a series of events that ultimately result in necrosis or apoptosis. The generation of harmful oxygen and nitrogen free radicals, depolarization of the mitochondrial membrane, activation of caspase, and cellular toxicity are some of these downstream consequences [15,16].

Vicious cycle or cascade of excitotoxicity, oxidative stress and apoptosis

Excitotoxicity can trigger oxidative stress by disrupting calcium homeostasis, and both excitotoxicity and oxidative stress can converge to activate apoptotic pathways, ultimately leading to neuronal death. Activation of NMDARs results in intracellular $Ca2^+$ influx, resulting in the activation of neuronal nitric oxide synthase that causes mitochondrial oxidative stress and dysfunction. The following events sequentially trigger the mitochondrial apoptotic signal pathway, resulting in apoptosis increased membrane permeability, leakage of cytochrome C – an inner mitochondrial membrane protein into the cytosol, apoptosome assembly (Apaf-1, caspase-9, ATP), activation of Caspase-3, Cleavage of poly (ADP-ribose) polymerase, nuclear translocation of apoptosis-inducing factor, and DNA fragmentation, resulting the neuronal death (apoptosis). Thus, the formation of ROS causes oxidative stress, leading to the production of apoptosis-inducing factors which promote programmed cell death (apoptosis) and degeneration of neurons [13-15].

Targeting excitotoxicity

Glutamate antagonists bind to NMDARs and inhibit the binding of glutamate; further, calcium influx and excitotoxicity can be prevented. GluN2B-containing NMDARs tend to encourage neuronal death regardless of where they are found extra-synaptic or synaptic [17]. Research indicates that NMDARs carrying GluN2B speed up the development of neurodegeneration in several neurological conditions, including Parkinson's and Huntington's illnesses [18], multiple sclerosis, AD, traumatic brain damage, amyotrophic lateral sclerosis, epilepsy, cerebral ischemia, and schizophrenia. For this reason, extensive research is being carried out into creating GluN2B-selective NMDAR antagonists that are therapeutically beneficial. Ifenprodil is the only reported inhibitor that binds to the interface of the GluN1 and GluN2B heterodimer of NMDA. However, ifenprodil's human clinical study for stroke was withdrawn due to a high risk/benefit ratio brought on by greater dosages, causing adverse cardiovascular consequences at higher doses [19].

METHODS

In silico studies

Preparation of chemical library

After an extensive literature survey, a list of phytochemicals was sourced from the National Center for Biotechnology Information (NCBI) PubChem database. The two-dimensional (2D) or three-dimensional (3D) structure of the phytochemicals, and one reported inhibitor, ifenprodil, were retrieved in .sdf format from NCBI PubChem. MarvinSketch 15.9.7.0 was utilized for the conversion from .sdf format to .Mol format for molecular drug property prediction and ChemSketch for ligand preparation [20,21].

Molecular drug properties predictions [22-25]

Molecule's drug properties, such as Drug likeliness (Lipinski's Rule of five), used Molsoft drug likeliness software and molecular property prediction online server. Mutagenicity of the compound (Ames test), amount of drug absorbed in the intestine, and penetration of the compound in blood–brain barrier (BBB) were examined using the Online BBB Prediction server (version 0.90) with the Ada Boost algorithm and Molecular ACCess System fingerprint by SwissADME Tool server.

Selection of compound based on molecular docking

Retrieval of receptor [26]

The 3D Structure of the GluN2B subunit-containing NMDAR was downloaded from the Research Collaboratory for Structural Bioinformatics -Protein Data Bank (PDB) in '".pdb"' format. NMDA (PDB ID: 5EWJ) is a crystal structure of amino-terminal domains of NMDAR subunit GLUN1 and GLUN2B in complex with Ifenprodil. This structure was determined at a resolution of 2.77Å and deposited in the database by Pandit *et al*., NMDA glutamate receptor subunit GluN1 (residues 23-405) from Xenopus laevis contains Chain A and C, whereas NMDR subunit GluN2B (residues31-394) from Homo sapiens consists of Chain B and D. The ifenprodil inhibitor binds at GluN2B ATDs heterodimer interface.

Discovery studio, PyRx, and other Docking tools [27]

Discovery Studio is a cutting-edge software tool that is commonly utilized in the molecular docking process. It also used to visualize all the interactions between the drug and all possible bindings with the amino acids of receptors in 2D and 3D form. The *in silico* investigation was carried out using offline programming tools such as the PDB, the PubChem database, and the Marvin sketch, which were also utilized. In the molecular docking research, PyRx 0.9 was employed. The Marvin sketch tool was used to create the ligands, and the molecules were constructed in two and three dimensions. Following the design, the structures were optimized in 3D in Marvin Sketch and saved as a.pdb file. PyRx was utilized for molecular docking and assessing the ligand and protein binding affinity.

Protein preparation

The optimized protein was saved in the ".pdbqt" format and imported into PyRx for molecular docking to demonstrate the bonds formed between the ligand tangeretin and 5EWJ as a potential therapeutic target for inhibiting the excitotoxicity pathway and neuronal apoptosis, to attain neuroprotective action.

Generation of ligands

The reported compound and depicted compound's 2D arrangement was generated through the utilization of ChemSketch software. To create a 3D structure from 2D ligand molecules, ligands were also loaded into ChemDraw. The resulting 3D ligands were saved as '".Mol" files. Utilizing the universal force field, the ligands were stabilized and optimized.

Molecular docking studies

In PyRx, the binding site was defined using the coordinates of the co-crystallized inhibitor, ifenprodil, bound to the NR2B subunit in the crystal structure of 5EWJ. The centroid of the ifenprodil coordinates was used to generate the docking grid, ensuring accurate coverage of the allosteric inhibitor pocket. Molecular docking was performed using AutoDock Vina implemented in PyRx 0.8. The grid box parameters were set with center coordinates at X: 83.3052, Y: 13.3273, Z: –41.6218 and dimensions (Å) of X: 65.7569, Y: 78.8265, Z: 86.9073. Docking poses were clustered using a 2.0 Å RMSD threshold to distinguish unique binding conformations. Non-bonded polar and hydrophobic interactions at the allosteric inhibitor site of protein (PDB ID:5EWJ) were modeled using Discovery Studio 2020 Client software. Ligands were then demonstrated by predicted interactions with the key amino acids that exist in the protein's region, which are then visualized in 2D and 3D forms using Discovery Studio.

In vitro studies

C6 cell line [28]

The cell line was obtained from the National Centre for Cell Sciences, Pune, India. A glioma-affected rat's brain was used to isolate the glial cell line C6.

- Organism: *Rattus norvegicus* (rat)
- Cell type: Adherent
- Tissue: Brain
- Disease: Glioma
- Applications: Neuroscience and toxicology.

Maintenance of C6 cell lines [29]

The C6 cells are maintained in 100 mm^2 tissue culture Petri dish in Ham's F12 Nutrient Mixture supplemented with 10% inactivated Fetal Bovine Serum (FBS), penicillin (100 IU/mL), streptomycin (100 µg/mL), and amphotericin B (5 µg/mL) with 10% FBS in incubator at 37°C with 5 % carbon dioxide (CO_2). The media to be changed every 48 h. Trypsin-ethylenediaminetetraacetic acid (EDTA) solution was used to dissociate and separate the cells. Split the cells in new tissue culture Petri dish when the cells reach 80–90% confluency.

MTT assay [30]

Extraction and filtration

Tangeretin is poorly soluble in culture media. Hence, 10 mg of the drug will be weighed, dissolved in 100 µL of dimethyl sulfoxide (DMSO), vortexed, and 900 µL of Ham's F-12 Nutrient Mixture medium without serum will be used to mix it well to obtain a stock solution of 10 mg/mL. Furthermore, a serial two-fold dilution was prepared from the stock solution to prepare lower concentrations for cytotoxicity testing and gene expression analysis.

Preparation and treatment of 96-well tissue culture plate

From the culture flask, cell monolayer was trypsinized and the cell count was adjusted to 1,00,000 cells/ML using Ham's F-12 Nutrient mixture containing 10% FBS. After trypsinization, the cells were seeded. About 100 µL concentration of the cells (about 10,000 cells) was added into each well and the plate was incubated for 24 h at 37°C with 5% CO_2. Once a partial monolayer had developed after 24 h of incubation, the supernatant was discarded, the monolayer was once again cleaned with Dulbecco's Phosphate-Buffered Saline, and various test concentrations were applied to the 96-well microtiter plates. Drug will be diluted up to eight different concentrations by a factor of two-fold dilution (1000 µg–7.8 µg) using media. The untreated cells were maintained as a cell control for comparison. Wells were filled with 100 µL of drug dilutions, and it was incubated for 24 h at 37°C with 5% CO_2. After 24 h, the medium will be decanted. Each well will be added with 50 µL of MTT and incubated for about 3 h at 37°C. It is covered with a foil covering and kept dark. Following a 3 h duration, MTT will be descanted, followed by the addition of 100 µL of DMSO, and microplate reader is used to scan the plate at 570 nm. The following formula is used to compute the proportion of viable cells:

$$\% \text{ of Cell viability} = \frac{\text{Optical density (a)}}{\text{Optical density (b)}} \times 100$$

a - Optical density of test sample; b - Optical density of Control.

Apoptosis assay [31-33]

An apoptosis assay is used to count the number of cells that have undergone apoptosis. This is done by initially staining the cells using Annexin V ($Ca2^+$-dependent phospholipid-binding protein with high affinity for PS) and propidium iodide (red-fluorescent nuclear and chromosome counterstain), further by flow cytometry analysis. A 6-well plate was seeded with cells at a density of 3 × 105 cells in 2 mL and then left for incubation at 37°C for 24 h in a CO_2 incubator overnight [31]. Spent media was removed and the cells were exposed to the necessary concentration of experimental compounds and controls in 2 mL of culture medium and then left to incubate for 24 h. Following treatment, the medium was discarded and the wells were rinsed with PBS buffer (pH 7.4). Subsequently, 200 µL of trypsin-EDTA solution was applied and allowed to incubate at 37°C for 3–4 min. Next, 2 mL culture medium was introduced and the cells were collected into 12 × 75 mm polystyrene tubes (6 tubes). The tubes were centrifuged for 5 min at 300× g at 25°C. The supernatant was carefully removed and the cells were washed twice with PBS before completely discarding the PBS solution. Following this, 5 µL of FITC Annexin V was added and incubated for 15 min at room temperature (25°C) in the dark. In addition, 5 µL of propidium iodide and 400 µL of 1X Binding Buffer were introduced into each tube and gently vortexed. Finally, the analysis was carried out in flow cytometry. Data analysis was performed using done using BD Cell Quest Pro Software (Version: 6.0). After acquisition was completed with BD Fluorescence Activated Cell Sorting (FACS) caliber. Here, the secondary fluorescence marker is propidium iodide and primary marker is Annexin V-FITC. The percentages of live, early apoptotic, late apoptotic, and necrotic cells were provided as the analysis's findings.

Gene expression [34]

The apoptotic genes that will be checked for quantitative expression are Bcl-2, Bax-2, Caspase-3, and poly(ADP-ribose) polymerase 1 (PARP-1).

RNA isolation [35]

Mix the collected pellets with 1 mL of RNA isoplus and mix thoroughly using pipettes and let them stand at room temperature for 5 min to extract RNA from the cells. Add 1 mL of chloroform to the mixture and mix well, allowing it to settle for 2–5 min. Then centrifuged at 4000 rpm for 10 min, leading to the formation of three layers (RNA on the top, DNA in the middle, and proteins and cell debris at the bottom). Hence, only the top RNA layer is carefully transferred into a tube containing equal proportion of isopropanol and mixed. Place the tubes are kept in a −20°C freezer for at least 30 min so as to increase the precipitation of RNA. The above solution is centrifuged at 10000–12000 rpm for 20 min. By the addition of isopropanol, the RNA will be precipitated and thus it settles down. Wash the RNA pellets by resuspending them in 75% ethanol and then the solution is centrifuged at about 7500 rpm for 20 min. Supernatant is discarded and the pellets are air dried till all the traces of ethanol evaporate.

Complementary DNA (cDNA) Preparation [36]

RNA pellets are resuspended by using nuclease-free water (30 µL) and transferred to polymerase chain reaction (PCR) tubes. cDNA master mix is added in an equal amount and placed in the PCR machine for the conversion of RNA to cDNA.

DNA amplification [37]

The cDNA synthesized was amplified by reverse transcription-PCR (RT-PCR) for Bax, Bcl2, PARP, and Caspase gene as well as glyceraldehyde-3-phosphate dehydrogenase (GAPDH) (used as internal control) transcripts. The expression levels of four genes were assessed through semi-quantitative RT-PCR. A 20 µL reaction mixture was prepared and utilized for PCR amplification of genes using cDNA and primers specifically designed and obtained from Eurofins, India. In addition, GAPDH (Housekeeping gene) was co-amplified with each reaction for internal control. The amplification solution is prepared and this composition is taken in PCR tubes and each of the tubes is marked consequently before being placing in the PCR machine. To initiate the amplification process, insert the PCR tubes containing the master mix along with the cDNA template into the PCR.

Primer used

Primers specific to the gene of interest were designed for Bax-2, Bcl-2, PARP-1, and caspase-3 gene and GAPDH using NCBI primer blast.

Gene expression

The relative messenger RNA (mRNA) expressions were quantified using 2-ΔΔCt method, which involved normalization to GAPDH.

RESULTS

Based on the suitability for Lipinski's rule of five (distinguishes between the drug-like and non-drug-like molecules) and docking scores compared with that of the ifenprodil (reported inhibitor), from the chemical library, the top one compound was chosen as a molecule of interest. Further, the membrane permeability and absorption, distribution, metabolism, excretion, and toxicity properties were analyzed.

Drug profile

- Drug Name: Tangeretin
- Molecular formula: $C_{20}H_{20}O_7$
- Molecular weight: 372.4 g/mol

NMDAR docking results

Ifenprodil 2D and 3D interaction with different amino acids present on the binding site of NMDAR

Figure 1 and Table 1.

Tangeretin 2D and 3D interaction with different amino acid present on the binding site of NMDAR

Figure 2 and Table 1

Molecular drug properties

Drug-likeliness prediction (Lipinski's rule of five), ADME prediction and toxicity prediction

Table 2.

MTT assay

Table 3.

Apoptosis assay

Figure 3, Table 5.

Gene expression study

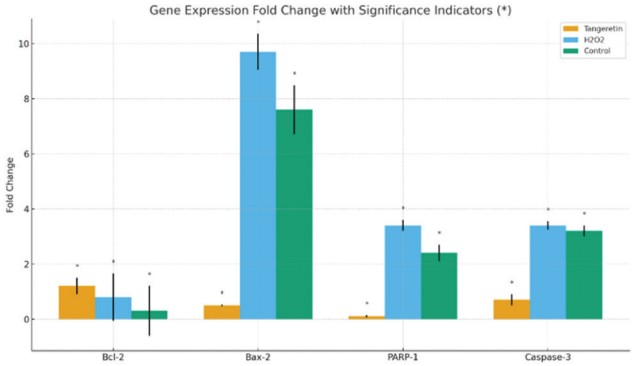

Data are presented as mean±standard deviation (n=3). Asterisks (*) above the bars indicate statistically significant differences ($p<0.05$) for the following comparisons: Tangeretin versus control, tangeretin versus hydrogen peroxide (H_2O_2), and H_2O_2 versus control for each gene. All gene expression values are normalized to GAPDH.

DISCUSSION

Ifenprodil binds at the GluN2B subunit involving binding with MET 207, ASP 211, ASP 210, LEU 209, PRO 340, THR 233, GLU 235, THR 333, GLU 106, GLU 236, ARG 115, ALA 107, ILE 335, TYR 239, and PHE 113 as shown in the 2D interaction (Fig. 1), mediating allosteric inhibition. The ligands were docked at the interface between Chain A and B, containing the GluN2B subunit, to determine the binding interactions. The bond energy Kcal/Mol was used to determine the binding energy; the lower the energy more stable the bond will be formed and vice versa. With the docking score of −7.3 against NMDA, tangeretin is projected to have a strong predicted binding affinity that that of other compounds and can be chosen as molecule of interest. Results have shown that tangeretin can allosterically inhibit the GluN2b subunit of NMDARs by binding at the subunit similar to the binding of ifenprodil. It was showing 10 Van der Waals bonds, MET 207, LEU 209, ASP210, ASP 211, ASN 334, GLU 235, THR 333, GLU 236, THR 233, GLU 106, 1 Conventional Hydrogen bond ARG 115, 2 pi-alkyl bonds, and 1 pi-pi T-shaped bond TYR 239 as shown in Table 1 and Fig. 2. The Lipinski's rule of five distinguishes between the drug-like and non-drug-like molecules. Tangeretin does not violate Lipinski's rule, indicating it is a good drug candidate (Table 2). Ames's test is a method to test mutagenicity as given by Dr. Ames. Tangeretin is predicted to be a non-mutagen and to have high gastrointestinal absorption (98.478%), so it can be used as an oral drug (Table 3). Tangeretin is also predicted to cross BBB+ which was interpreted by the Swiss ADME Model (Boiled Egg prediction). Hence, it can be used for treating neurodegenerative diseases. Statistical analysis of the MTT assay data revealed that tangeretin did not exhibit strong cytotoxicity against the C6 glioma cell line within the tested concentration range (7.81–1000 µg/mL). Although a dose-dependent decrease in cell viability was observed, the reduction was modest. At the highest concentration (1000 µg/mL), tangeretin produced 85.65±1.07% cell viability. The CTC50 value of the test substance on the Rat Glioma (C6) cell line was above 1000 µg/mL (Table 3). Accordingly, the safe dosage form was chosen for further research, i.e., 1000 µg/mL and 500 µg/mL, in these dilutions, a negligible amount of cell metabolites was found, and cells were not in a stress condition. Consequently, an apoptosis assay was performed using these two dilutions. According to the FACs data by flow cytometry, the percentage of early apoptotic and late apoptotic cells decreased in the treated group of tangeretin, when compared to that of the early and late apoptotic cells of control cells. % Apoptosis in 500 µg tangeretin-treated cells was only 2.04 when compared to the positive control (doxorubicin-treated cells) and cell control. Even though in 1000 µg tangeretin treated cells % apoptotic cells has increased to 10.14 compared to the cell control, it is lower compared to the positive control. Thus, tangeretin at 500 µg concentration has a higher anti-apoptotic effect (Fig. 3). Tangeretin has shown positive findings in the apoptosis assay, but its effect on various genes involved in apoptosis needs to be assessed. The members of the Bcl-2 family, which includes Bax and Bcl-2 as well as Caspase-9/3, are involved in apoptosis. Thus, modulation of apoptosis-related genes may be protective against apoptosis, which is one of the therapeutic strategies in neurodegenerative diseases (Table 4). Quantitative RT-PCR analysis revealed the modulatory effect of tangeretin on the mRNA expression of all four apoptotic genes over the standard and cell control. The expression of Bcl-2 mRNA, which is an indicator of the level of anti-apoptosis, was increased in the tangeretin-treated cells compared to the standard-H_2O_2 (Fig. 4, Table 5). In contrast, the expression of Bax-2, PARP-1, and Caspase-3 mRNA, which are indicators of the level of pro-apoptosis, was increased in the standard-treated cells and decreased in the tangeretin-treated cells. The amplification curve of test products indicates the expression of Bcl-2, Bax-2, Caspase-3, and PARP-1 according to the Ct values. The Ct values of tangeretin represent the effect of the product being higher for Bcl-2 gene

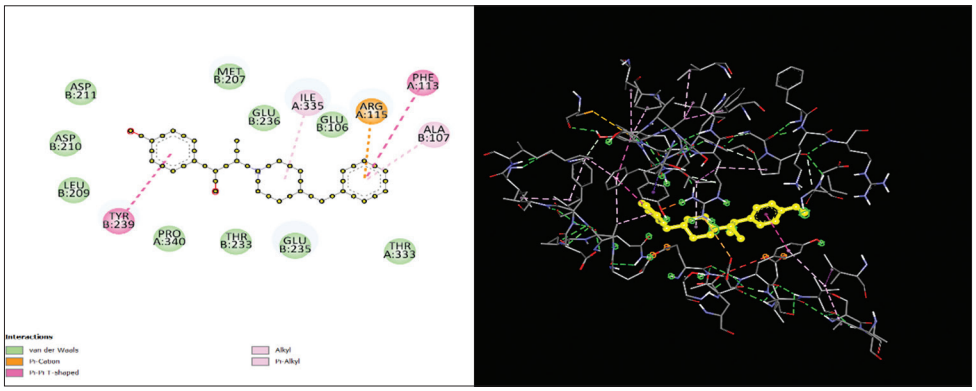

Fig. 1: Ifenprodil two-dimensional and three-dimensional interaction with N-methyl-D-aspartic acid receptor

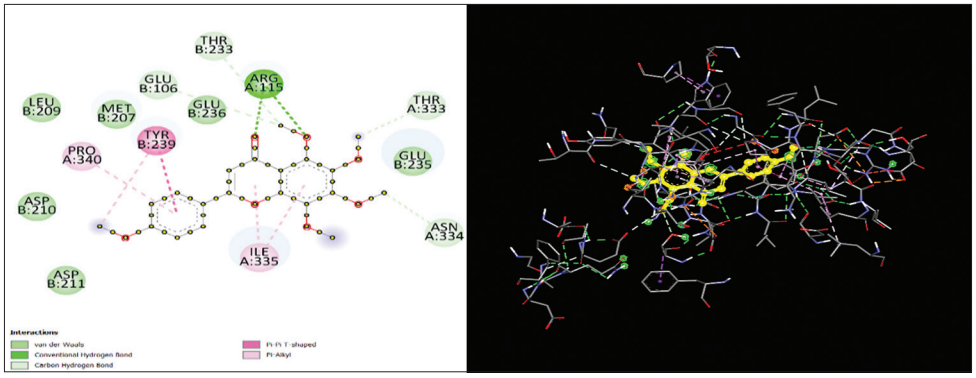

Fig. 2: Tangeretin two-dimensional and three-dimensional Interaction with N-methyl-D-aspartic acid receptor

Table 1: Binding affinity, amino acid position, and types of interactions of ifenprodil and tangeretin with N-methyl-D-aspartic acid receptor

S. No.	LIGANDS	Docking score (kcal/mol)	Types of interaction	Aminoacids and their positions
1.	Ifenprodil	-7.5	Van der Waals	MET 207, ASP 211, ASP 210, LEU 209, PRO 340, THR 233, GLU 235, THR 333, GLU 106, GLU 236
			PiCation	ARG 115
			Alkyl	ALA 107
			Pi- Alkyl	ILE 335
			Pi-Pi T-Shaped	TYR 239, PHE 113
2.	Tangeretin	-7.3	Van der Waals	MET 207, LEU 209, ASP210, ASP 211, ASN 334, GLU 235, THR 333, GLU 236, THR 233, GLU 106
			Conventional hydrogen bonds	ARG 115
			Pi-Alkyl	ILE 335, PRO 340
			Pi-Pi T-Shaped	TYR 239

Table 2: Tangeretin – Lipinski's rule of five, ADME properties, retrieved from SwissADME, and toxicity data retrieved from PKSM online server for the molecule

S. No.	Properties	Results
1.	Molecular weight	372.12 (≤500 Daltons)
2.	Hydrogen bond acceptors	7 (≤ 10)
3.	Hydrogen bond donors	0 (≤5)
4.	MolLogP	4.23 (≤5)
5.	MolLogS	−4.80
6.	GI absorption	High (according to the white of the boiled egg) 98.478% (%absorbed)
7.	BBB Permeant	YES (according to the Yolk of the boiled egg) 1.026 (log BB) (readily cross the blood–brain barrier)
8.	Ames toxicity	Negative (No mutation)
9.	Hepatotoxicity	Negative
10.	Skin sensitization	Negative

BBB: Blood–brain barrier, ADME: Absorption, distribution, metabolism, excretion

Table 3: *In vitro* cytotoxicity of tangeretin in terms of percentage cell viability against rat glioma (C6) cell line by MTT assay

Test substance	Concentration (µg/mL)	Percentage of cell viability after treatment (Mean±SD)
Tangeretin	1000	85.65±1.07
	500	86.59±1.55
	250	87.20±1.67
	125	91.45±3.26
	62.5	93.10±2.70
	31.25	93.03±2.79
	15.62	95.67±2.95
	7.81	98.34±1.80

Values represent mean±SD (n=3). Statistical analysis was performed using one-way ANOVA followed by Tukey's *post hoc* test. A significant reduction in cell viability compared with control was observed only at 1000 µg/mL ($p<0.05$). ANOVA: Analysis of variance, SD: Standard deviation

Table 4: Percentage apoptosis by tangeretin in C6 cell line by flow cytometry analysis

Test samples	% Apoptotic cells (Early+Late apoptosis)
Cell control	2.25
Positive control (Doxorubicin)-500 µg	31.89
Positive control (Doxorubicin)-1000 µg	87.57
0794 (Tangeretin)-500 µg	2.02
0794 (Tangeretin)-1000 µg	9.12

expression compared to the other three genes. In contrast, the near-complete suppression of PARP-1 expression is striking and suggests a strong inhibitory effect on a key DNA-damage-associated apoptotic pathway. Although this finding aligns with the observed reduction in apoptosis, the exact mechanism remains unclear. Whether tangeretin directly modulates PARP-1 or indirectly affects upstream oxidative stress pathways is unknown and requires further mechanistic studies. When compared with the cell control and standard, the tangeretin treatment group showed increases in the levels of Bcl-2 by 1.0-fold at 1000 µg/mL concentrations when compared with the standard-H_2O_2 (0.6-fold). It is important to note that the C6 rat glioma (glial) cell line is not a neuronal cell line and does not express functional NMDARs at levels comparable to cortical or hippocampal neurons. It is often used in preliminary neuroprotection studies due to its stable growth and expression of basic apoptotic machinery. However, the translation of these findings

Table 5: The quantitative expression level of *Bcl-2, Bax-2, Caspase-3,* and *PARP-1 g*enes normalized to GAPDH in terms of expression fold

S. No.	Test sample	Regulation in terms of expression folds			
		Bcl-2	Bax-2	PARP	Caspase-3
1.	Tangeretin-1000 µg/mL	1.2±0.3	0.5±0.03	0.1±0.04	0.7±0.2
2.	Standard-H_2O_2 1000 µg/mL	0.8±0.86	9.7±0.65	3.4±0.2	3.4±0.15
3.	Cell control	0.3±0.9	7.6±0.89	2.4±0.3	3.2±0.2

Data are expressed as mean±SD (n=3). Gene expression levels were quantified using quantitative reverse transcription and normalized to glyceraldehyde-3-phosphate dehydrogenase. Statistical significance was determined for tangeretin versus control, tangeretin versus H2O2, and H2O2 versus control ($p<0.05$), corresponding to the significance indicators shown in the accompanying figure. GAPDH: Glyceraldehyde-3-phosphate dehydrogenase, PARP1: Poly (ADP-ribose) polymerase 1, SD: Standard deviation, H2O2: Hydrogen peroxide

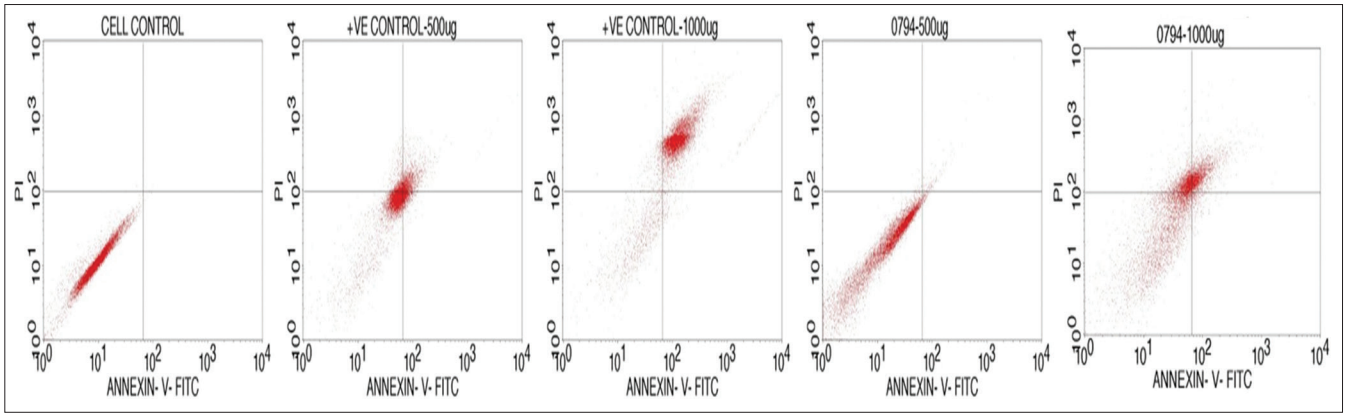

Fig. 3: Quadrangular plots represented the Annexin V/PI expression in C6 cells in the presence and absence of tangeretin by flow cytometry. Acquisition was done by using BD FACS Caliber and data analyzed by BD Cell Quest Pro Software (Version: 6.0). Here, Annexin V-FITC - Primary Marker, PI - Propidium Iodide (Secondary fluorescence Marker). *0794-Tangeretin

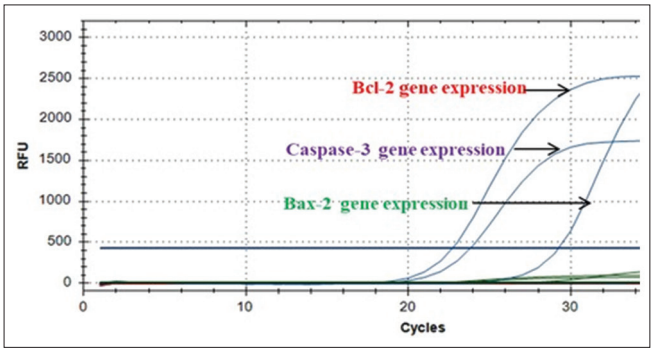

Fig. 4: Amplification curve of Tangeretin on the quantitative gene expression level of Bcl-2, Bax-2, Caspase-3, and poly(ADP-ribose) polymerase 1 (amplification curve not observed) transcripts in rat glioma (C6) cell line, normalized to glyceraldehyde-3-phosphate dehydrogenase

to a neuronal context is limited, and future studies must use neuronal or induced pluripotent stem cell-derived neuronal models to validate NMDAR-related effects.

CONCLUSION

The present study was performed to identify and analyze the neuroprotective activity of a potent phytochemical, which was initiated with *in silico* studies and prediction of molecular drug properties, and tangeretin was selected from the ligand dataset. To evaluate its neuroprotective effect, our study hypothesized NMDAR inhibition as a potential strategy to attenuate neuronal apoptosis (neurodegeneration). Tangeretin was predicted to have good binding affinity in the interface of the GluN2B subunit containing the NMDAR. Tangeretin can be used as an oral drug because it has high GI absorption and also it is BBB-positive. Further, *in vitro* studies were executed by MTT to obtain two higher non-toxic concentrations of tangeretin. These concentrations were evaluated on the targets for the neuroprotection study. Apoptosis assay helps to identify the neurodegeneration activity and levels of genes that are expressed are determined by Gene expression studies. Apoptosis assay and gene expression showed that tangeretin at 500 µg/ml concentration did not show a significant rate of apoptosis, whereas at 1000 ug/ml concentration caused a moderate rate of apoptosis in rat glioma (C6) cell lines, which shows that tangeretin has a neuroprotective effect. Tangeretin increases Bcl-2, an anti-apoptotic gene. Furthermore, tangeretin subsequently showed a significant decrease in Bax-2, Caspase-3, and PARP-1, which are pro-apoptotic genes, thus preventing apoptosis, which plays a major role in the pathogenesis of neurodegenerative diseases. These findings support the possibility that tangeretin may exert cytoprotective actions through modulation of apoptotic pathways. By elucidating the molecular interactions, cellular pathways, and physiological responses associated with tangeretin treatment, we have laid the groundwork for further exploration and development of tangeretin-based neuroprotective interventions. These findings indicate that tangeretin may serve as a promising and safe therapeutic option for the treatment of neurodegenerative diseases. Future work must include neuronal cell models, dose-response gene expression studies, and direct functional assays of NMDAR activity to validate its mechanism and therapeutic relevance. With further investigation, tangeretin may emerge as a promising scaffold for developing neuroprotective interventions.

ACKNOWLEDGMENTS

The authors would like to thank JSS College of Pharmacy, JSS Academy of Higher Education and Research, Mysuru, for their support.

CONFLICT OF INTEREST

The authors declare that there is no conflict of interest.

FUNDING

None.

DATA AVAILABILITY

All datasets generated or analyzed during this study are included in the manuscript.

ETHICS STATEMENT

Not applicable.

INFORMED CONSENT STATEMENT

Not applicable.

REFERENCES

1. Safitri I, Hidayati HB, Turchan A, Suhartati KS, Khaerunnisa S. *Solanum betaceum* improves cognitive function by decreasing N-methyl-D-aspartate in Alzheimer rat model. Int J Appl Pharm. 2019;11:167-70. doi: 10.22159/ijap.2019.v11s5.T1015
2. Cannon JR, Greenamyre JT. The role of environmental exposures in neurodegeneration and neurodegenerative diseases. Toxicol Sci. 2011 Dec;124(2):225-50. doi: 10.1093/toxsci/kfr239, PMID 21914720
3. Przedborski S, Vila M, Jackson-Lewis V. Neurodegeneration: What is it and where are we? J Clin Invest. 2003 Jan;111(1):3-10. doi: 10.1172/jci17522, PMID 12511579
4. Neurological Disorders Affect Millions Globally: WHO Report; 2007. World Health Organization. Available from: https://www.who.int/news/item/27-02-2007-neurological-disorders-affect-millions-globally-who-report
5. World Health Organization. Dementia; 2025 Mar 31. Available from: https://www.who.int/news-room/fact-sheets/detail/dementia
6. El-Assal MI, Samuel D. Optimization of rivastigmine chitosan nanoparticles for neurodegenerative Alzheimer; *in vitro* and *ex vivo* characterizations. Int J Pharm Pharm Sci. 2022;14:17-27. doi: 10.22159/ijpps.2022v14i1.43145
7. Ding C, Wu Y, Chen X, Chen Y, Wu Z, Lin Z. Global, regional, and national burden and attributable risk factors of neurological disorders: The Global burden of disease study 1990-2019. Front Public Health. 2022;10:952161. doi: 10.3389/fpubh.2022.952161, PMID 36523572
8. Connolly BS, Lang AE. Pharmacological treatment of Parkinson disease: A review. JAMA. 2014;311(16):1670-83. doi: 10.1001/jama.2014.3654, PMID 24756517
9. Jann MW, Shirley KL, Small GW. Clinical pharmacokinetics and pharmacodynamics of cholinesterase inhibitors. Clin Pharmacokinet. 2002;41(10):719-39. doi: 10.2165/00003088-200241100-00003, PMID 12162759
10. Golechha M, Sarangal V, Bhatia J, Chaudhry U, Saluja D, Arya DS. Naringin ameliorates pentylenetetrazol-induced seizures and associated oxidative stress, inflammation, and cognitive impairment in rats: Possible mechanisms of neuroprotection. Epilepsy Behav. 2014;41:98-102. doi: 10.1016/j.yebeh.2014.09.058, PMID 25461197.
11. Lindvall O, Kokaia Z. Prospects of stem cell therapy for replacing dopamine neurons in Parkinson's disease. Trends Pharmacol Sci. 2009;30(5):260-7. doi: 10.1016/j.tips.2009.03.001, PMID 19362379
12. Livingston G, Huntley J, Sommerlad A, Ames D, Ballard C, Banerjee S. Dementia prevention, intervention, and care: 2020 Report of the lancet commission. Lancet. 2020;396(10248):413-46. doi: 10.1016/S0140-6736(20)30367-6, PMID 32738937
13. Robinson MT, Holloway RG. Palliative care in neurology. Mayo Clin Proc. 2017;92(10):1592-601. doi: 10.1016/j.mayocp.2017.08.003, PMID 28982489
14. Sasidharan A, Deepthi K, Dixit S, Singh D, Tom VV, Somayaji Y. *In silico* evaluation of CSF1R inhibitors: A promising approach for targeting neuroinflammation in neurodegenerative diseases. Int J Appl Pharm. 2025;17:268-80. doi: 10.22159/ijap.2025v17i2.53425
15. Kalia LV, Lang AE. Parkinson's disease. Lancet. 2015;386(9996):896-912. doi: 10.1016/S0140-6736(14)61393-3, PMID 25904081
16. Zakiya Fathima C, James JP, Srinivasa MG, Sindhu TJ, Mariyam Jouhara BM, Revanasiddappa BC. Investigating multitarget potential of *Mucuna pruriens* against Parkinson's disease: Insights from molecular docking, MMGBSA, pharmacophore modelling, MD simulations and ADMET analysis. Int J Appl Pharm. 2024;16:176-93. doi: 10.22159/ijap.2024v16i5.51474
17. Ahmad K, Baig MH, Gupta GK, Kamal MA, Pathak N, Choi I. Identification of common therapeutic targets for selected neurodegenerative disorders: An *in silico* approach. J Comput Sci. 2016;17:292-306. doi: 10.1016/j.jocs.2016.03.007
18. Siafaka PI, Okur ME, Üstündağ Okur N. Editorial: Innovative therapies against neurodegenerative disorders: From new active molecules to novel drug delivery systems. Front Pharmacol. 2025;16:1640758. doi: 10.3389/fphar.2025.1640758, PMID 40635745
19. Roy S, Awasthi H. Herbal medicines as neuroprotective agent: A mechanistic approach. Int J Pharm Pharm Sci. 2017;9(10):1-7. doi: 10.22159/ijpps.2017v9i11.19444
20. Alov P, Stoimenov H, Lessigiarska I, Pencheva T, Tzvetkov NT, Pajeva I. *In silico* identification of multi-target ligands as promising hit compounds for neurodegenerative diseases drug development. Int J Mol Sci. 2022;23(21):13650. doi: 10.3390/ijms232113650, PMID 36362434
21. Islam MT, Aktaruzzaman M, Barai C, Rafi FI, Hasan AR, Tasnim T. *In silico* screening of naturally derived dietary compounds as potential butyrylcholinesterase inhibitors for Alzheimer's disease treatment. Sci Rep. 2025;15(1):17134. doi: 10.1038/s41598-025-98092-y, PMID 40382441
22. Swiss AD. SwissADME. Available from: https://www.swissadme.ch
23. Blood-Brain Barrier Predictor. Available from: https://www.cbligand.org/BBB/predictor.php [Last accessed on 2024 Apr 07].
24. PreADMET: ADME/Tox Prediction. Prediction of ADME/Tox; 2015. Available from: https://preadmet.webservice.bmdrc.org/adme-prediction
25. MolSoft LL. Drug-Likeness and Molecular Property Prediction. Available from: https://www.molsoft.com/mprop [Last accessed on 2024 Apr 07].
26. RCSB PDB. 5EWJ: Crystal Structure of Amino-Terminal Domains of the NMDA Receptor Subunit GluN1 and GluN2B in Complex with Ifenprodil. Available from: https://www.rcsb.org/structure/5EWJ [Last accessed on 2024 Apr 07].
27. Alqahtani T, Deore SL, Kide AA, Shende BA, Sharma R, Dadarao Chakole R. Mitochondrial dysfunction and oxidative stress in Alzheimer's disease, and Parkinson's disease, Huntington's disease and amyotrophic lateral sclerosis -an updated review. Mitochondrion. 2023;71:83-92. PMID 37269968
28. ATCC. C6 Cell Line Search. Available from: https://www.atcc.org/search#q=c6%20cell%20lines [Last accessed on 2024 Apr 08].
29. Benda P, Lightbody J, Sato G, Levine L, Sweet W. Differentiated rat glial cell strain in tissue culture. Science. 1968;161:370-1. PMID 4873531
30. Van Meerloo J, Kaspers GJ, Cloos J. Cell sensitivity assays: The MTT assay. Methods Mol Biol. 2011;731:237-45. doi: 10.1007/978-1-61779-080-5_20, PMID 21516412
31. Lakshmanan I, Batra SK. Protocol for apoptosis assay by flow cytometry using annexin V staining method. Bio Protoc. 2013;3(6):e374. doi: 10.21769/bioprotoc.374, PMID 27430005
32. Apoptosis Protocols. USF Health. Available from: https://health.usf.edu/medicine/corefacilities/flowcytometry/methods-apoptosis [Last accessed on 2024 Apr 09].
33. Bellavite P. Neuroprotective potentials of flavonoids: Experimental studies and mechanisms of action. Antioxidants (Basel). 2023;12(2):280. doi: 10.3390/antiox12020280, PMID 36829840
34. Barber RD, Harmer DW, Coleman RA, Clark BJ. GAPDH as a housekeeping gene: Analysis of GAPDH mRNA expression in a panel of 72 human tissues. Physiol Genomics. 2005;21(3):389-95. doi: 10.1152/physiolgenomics.00025.2005, PMID 15769908
35. Chomczynski P, Sacchi N. Single-step method of RNA isolation by acid guanidinium thiocyanate-phenol-chloroform extraction. Anal Biochem. 1987;162(1):156-9. doi: 10.1006/abio.1987.9999, PMID 2440339
36. Gubler U, Hoffman BJ. A simple and very efficient method for generating cDNA libraries. Gene. 1983;25(2-3):263-9. doi: 10.1016/0378-1119(83)90230-5, PMID 6198242.
37. Bustin SA, Benes V, Garson JA, Hellemans J, Huggett J, Kubista M. The MIQE guidelines: Minimum information for publication of quantitative real-time PCR experiments. Clin Chem. 2009;55(4):611-22. doi: 10.1373/clinchem.2008.112797, PMID 19246619